J Electr Eng Technol Vol. 9, No. 6: 1960-1966, 2014
http://dx.doi.org/10.5370/JEET.2014.9.6.1960

ISSN(Print) 1975-0102
ISSN(Online) 2093-7423

Analysis of a Surface-Mounted Permanent-Magnet Machine with Overhang Structure by Using a Novel Equivalent Magnetic Circuit Model

Han-Kyeol Yeo*, Dong-Kyun Woo, Dong-Kuk Lim*, Jong-Suk Ro† and Hyun-Kyo Jung***

Abstract – The rotor overhang is used to enhance the air-gap flux and improve the power density. Due to the asymmetry in the axial direction caused by the overhang, a time consuming 3D analysis is necessary when designing a motor with overhang. To solve this problem, this paper proposes an equivalent magnetic circuit model (EMCM) which takes account overhang effects without a 3D analysis by using effective air-gap length. The analysis time can be reduced significantly via the proposed EMCM. A reduction in the analysis time is essential for a preliminary design of a motor. In order to verify the proposed model, a 3-D finite-element method (FEM) analysis is adopted. 3-D FEM results confirm the validity of the proposed EMCM.

Keywords: Analytical method, Equivalent magnetic circuit model, Rotor overhang, SPM machine

1. Introduction

Permanent-magnet (PM) brushless machines are increasingly being used in various applications, such as electric vehicles, industrial servos and in wind power generation systems [9]. This increased popularity is due to their high torque, high power density, high efficiency, and low maintenance requirements as a consequence of the use of PM materials in the rotor. Surface-mounted permanent-magnet (SPM) motors have the advantages of low torque ripple and low cogging torque as compared with interior permanent-magnet (IPM) machines.

The overhang is defined in this paper as a configuration that the rotor length is longer than the stator length in the axial direction. In general, the overhang structure is used to enhance the air-gap flux and improve the power density while utilizing the free space caused by the stator end winding [29]. A 3-D finite-element method (FEM) is necessary to analyze the magnetic fields in the axial direction for a proper consideration of the overhang effects. Although FEM can precisely obtain the magnetic flux distribution and electromagnetic performances of electrical machines [22-24], it is time consuming and computationally expensive, especially at pre-design stages.

To reduce computational time for the motor design process, analytical methods are essential during the preliminary design of electric machines. Two types of analytical methods are usually used. The first one is based on the formal solution of Maxwell's equations. It can calculate parameters and performances of electric machines with high accuracy [1-5, 8, 13, 15, 19-21, 27, 28, 30]. Also, this method can be used for analyzing practical electrical machines with the geometric complexity, such as synchronous reluctance motors [15], switched reluctance machines (SRM) [27], SPM machines [2, 4, 5, 30], slotless motors [19, 20], and PM actuator [13, 21]. The second method is an equivalent magnetic circuit model (EMCM). As an EMCM has the advantage of simplicity compared to the aforementioned method, it is widely used as an analytical method for various types of machines [6, 10-12, 14, 16-18, 25, 26, 31, 32], such as SPM machines [10, 12, 18], IPM machines [16, 31], flux-switching PM machines [32], SRM [25], axial flux PM motors [14, 17], and induction machines [26].

In the case of SPM motors, an EMCM required to predict the air-gap and magnet flux density analytically has been developed while taking into account the leakage flux around the magnets in the rotor [18]. However, overhang effects in SPM machines with rotor overhang are presently not included in the EMCM. In this paper, we propose an EMCM considering not only the leakage flux in the rotor but also the overhang effects for SPM machines with rotor overhang. A 3-D FEM analysis is used to verify the proposed model.

2. Analytical Model of SPM Machines with Overhang

Although the effects of the stator slots have been taken

† Corresponding Author: Creative Research Engineer Development, Brain Korea 21 Plus, Seoul National University, Seoul, Korea. (jongsukro@naver.com)
* Dept. of Electrical and Computer Engineering, Seoul National University, Korea. (gksruf88@snu.ac.kr)
** Power & Industrial Systems R&D Center, Hyosung Corporation, Anyang. (wdkyun@gmail.com)
Received: February 11, 2014; Accepted: May 28, 2014

into account [10-12, 14, 16-18, 25, 26, 32], an EMCM which disregards slotting effects was developed in order to focus on the overhang effects and simplify the analytical model in this paper. It is assumed that the effects of saturation within the core are negligible, as the magnetic flux density within the core is low in general and because normally there is no significant saturation.

With the motor topology generalized as the linear translation type shown in Fig. 1, it is possible to derive an EMCM applicable to any specific topology. In order to enhance the air-gap flux and improve the power density, the overhang structure is used in the linear translation motor here, as shown in Fig. 2.

Qu *et al*. developed an EMCM for SPM machines that takes into account the air-gap leakage fluxes around the magnets [18]. The air-gap leakage fluxes consist of the magnet-to-magnet leakage flux and the magnet-to-rotor leakage flux. With the circular-arc straight-line permeance model [7], these leakage fluxes were modeled. However, this analytical model cannot be applied to SPM motors with overhang because the overhang results in asymmetry of the magnetic fields in the axial direction.

An EMCM based on the analytical model developed by Qu *et al*. considering overhang effects as well as air-gap leakage fluxes is proposed. Fig. 3 shows the proposed EMCM. The variables shown in Fig. 3 are defined as follows:

Φ_g : the air-gap flux excited by one magnet pole
Φ_r : the flux source of one magnet pole
R_g : the reluctance corresponding to Φ_g
R_{mo} : the reluctance corresponding to Φ_r
R_r : the reluctance of the rotor yoke
R_s : the reluctance of the stator yoke
R_{mm} : the reluctance corresponding to the magnet-to-magnet leakage flux
R_{mr} : the reluctance corresponding to the magnet-to-rotor leakage flux.

R_r and R_s can be ignored due to the assumption mentioned earlier. Fig. 3 can be simplified into Fig. 4 through the use of symmetry. In Fig. 4, R_m is calculated from Fig. 3 as

$$R_m = \frac{R_{mo}}{1+2\eta+4\lambda}, \tag{1}$$

where

$$\eta = \frac{R_{mo}}{R_{mr}} \tag{2}$$

and

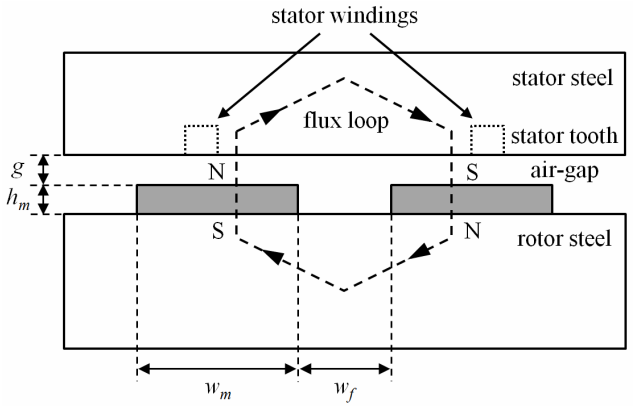

Fig. 1. Linear transfer motor topology

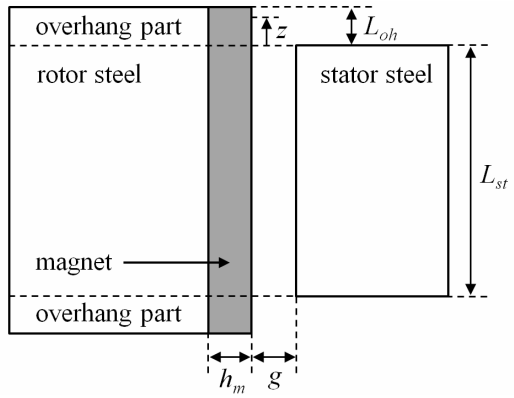

Fig. 2. Configuration of a motor with overhang

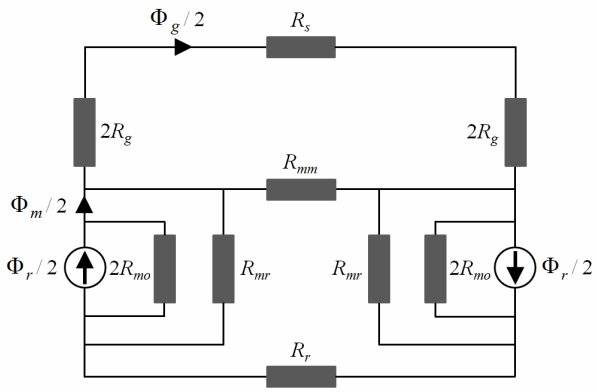

Fig. 3. Equivalent magnetic circuit for Fig. 1 and Fig. 2

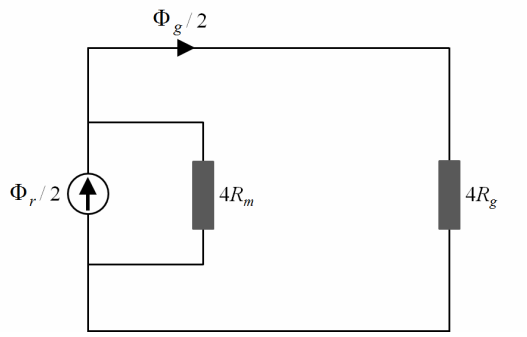

Fig. 4. Simplified circuit of Fig. 3

$$\lambda = \frac{R_{mo}}{R_{mm}}. \tag{3}$$

For the EMCM considering the overhang effect, the effective air-gap length should be defined. Flux lines between overhang structure and stator core are modeled with consideration for the distribution of magnetic flux density in the air gap. Fig. 5 shows modeling of flux lines in the air gap with a circular arc and a straight line. The magnetic flux distribution in the air gap which is calculated through FEM is shown in Fig. 6. The effective air-gap length is derived via the modeling of flux lines with a circular arc and a straight line as

$$g_e = \begin{cases} \sqrt{g^2 + z^2} & 0 < z \le g \\ \dfrac{\pi}{2} z & g < z \end{cases}, \tag{4}$$

where z is the position in the overhang, as shown in Fig. 5, and g is the air-gap length.

The permeances in the non-overhang region is derived in [18] as

$$P_g' = \frac{\mu_0 (w_m + \min(2g, w_f)) L_{st}}{g} \tag{5}$$

$$P_{mo}' = \frac{\mu_0 \mu_r w_m L_{st}}{h_m} \tag{6}$$

$$P_{mm}' = \frac{\mu_0 L_{st}}{\pi} \ln\left(1 + \frac{\pi \min(g, \frac{w_m}{2})}{w_f}\right) \tag{7}$$

$$P_{mr}' = \frac{\mu_0 L_{st}}{\pi} \ln\left[1 + \frac{\pi \min\left(g, \frac{w_f}{2}\right)}{h_m}\right], \tag{8}$$

where μ_0 is the permeability of air, μ_r is the magnet relative recoil permeability, L_{st} is the stator stack length, g is the air-gap length, w_f is the width between two adjacent magnets, w_m is the magnet width, h_m is the magnet length, and min(·) is the minimum function.

With the effective air-gap length g_e, the permeances of the infinitesimal stack length dz in the overhang can be derived. The permeances can be calculated by integrating

$$P_g'' = \begin{cases} \displaystyle\int_0^{L_{oh}} \frac{\mu_0 \left(w_m + \min\left(2\sqrt{g^2 + z^2}, w_f\right)\right)}{\sqrt{g^2 + z^2}} dz, & (g \ge L_{oh}) \\ \displaystyle\int_0^{g} \frac{\mu_0 \left(w_m + \min\left(2\sqrt{g^2 + z^2}, w_f\right)\right)}{\sqrt{g^2 + z^2}} dz + \int_g^{L_{oh}} \frac{2\mu_0 \left(w_m + \min(\pi z, w_f)\right)}{\pi z} dz, & (g < L_{oh}) \end{cases} \tag{9}$$

$$P_{mo}'' = \frac{\mu_0 \mu_r w_m L_{oh}}{h_m} \tag{10}$$

$$P_{mm}'' = \begin{cases} \displaystyle\int_0^{L_{oh}} \frac{\mu_0}{\pi} \ln\left(1 + \frac{\pi \min\left(\sqrt{g^2 + z^2}, \frac{w_m}{2}\right)}{w_f}\right) dz, & (g \ge L_{oh}) \\ \displaystyle\int_0^{g} \frac{\mu_0}{\pi} \ln\left(1 + \frac{\pi \min\left(\sqrt{g^2 + z^2}, \frac{w_m}{2}\right)}{w_f}\right) dz + \int_g^{L_{oh}} \frac{\mu_0}{\pi} \ln\left(1 + \frac{\pi \min\left(\frac{\pi z}{2}, \frac{w_m}{2}\right)}{w_f}\right) dz, & (g < L_{oh}) \end{cases} \tag{11}$$

$$P_{mr}'' = \begin{cases} \displaystyle\int_0^{L_{oh}} \frac{\mu_0}{\pi} \ln\left[1 + \frac{\pi \min\left(\sqrt{g^2 + z^2}, \frac{w_f}{2}\right)}{h_m}\right] dz, & (g \ge L_{oh}) \\ \displaystyle\int_0^{g} \frac{\mu_0}{\pi} \ln\left[1 + \frac{\pi \min\left(\sqrt{g^2 + z^2}, \frac{w_f}{2}\right)}{h_m}\right] dz + \int_g^{L_{oh}} \frac{\mu_0}{\pi} \ln\left[1 + \frac{\pi \min\left(\pi z/2, \frac{w_f}{2}\right)}{h_m}\right] dz, & (g < L_{oh}) \end{cases} \tag{12}$$

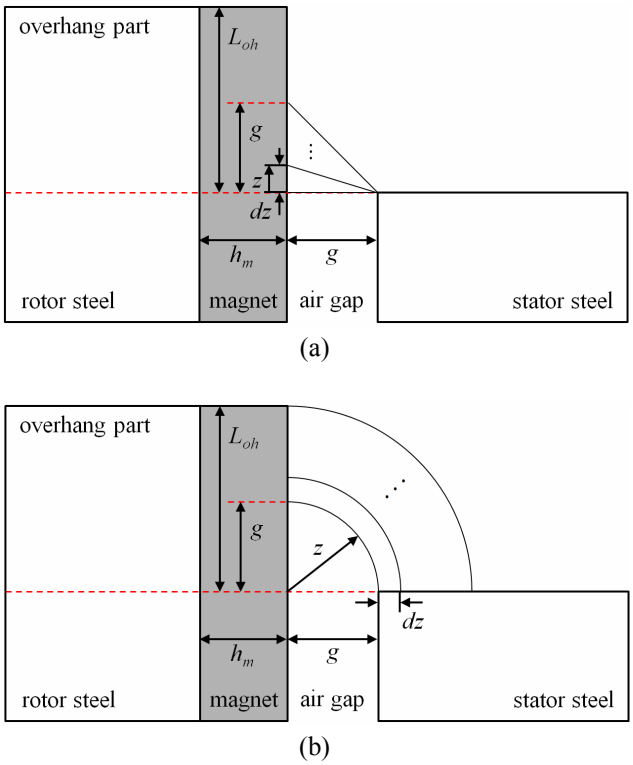

Fig. 5. Modeling of the flux lines in the air gap with a circular arc and a straight line: (a) A straight-line permeance model; (b) A circular-arc permeance model

the permeances of the infinitesimal stack length over the overhang length, as (9)-(12), where L_{oh} is the rotor overhang length.

With the permeances in the non-overhang region and the overhang region, the permeances for the entire motor with overhang are derived as follows:

$$P_g = P_g' + 2P_g'' \tag{13}$$

$$P_{mo} = P_{mo}' + 2P_{mo}'' \tag{14}$$

$$P_{mm} = P_{mm}' + 2P_{mm}'' \tag{15}$$

$$P_{mr} = P_{mr}' + 2P_{mr}'' . \tag{16}$$

Using the equations above and the reciprocal relationship between the permeance and reluctance, the reluctances are calculated as follows:

$$R_g = \frac{1}{P_g} \tag{17}$$

$$R_{mo} = \frac{1}{P_{mo}} \tag{18}$$

$$R_{mm} = \frac{1}{P_{mm}} \tag{19}$$

$$R_{mr} = \frac{1}{P_{mr}} . \tag{20}$$

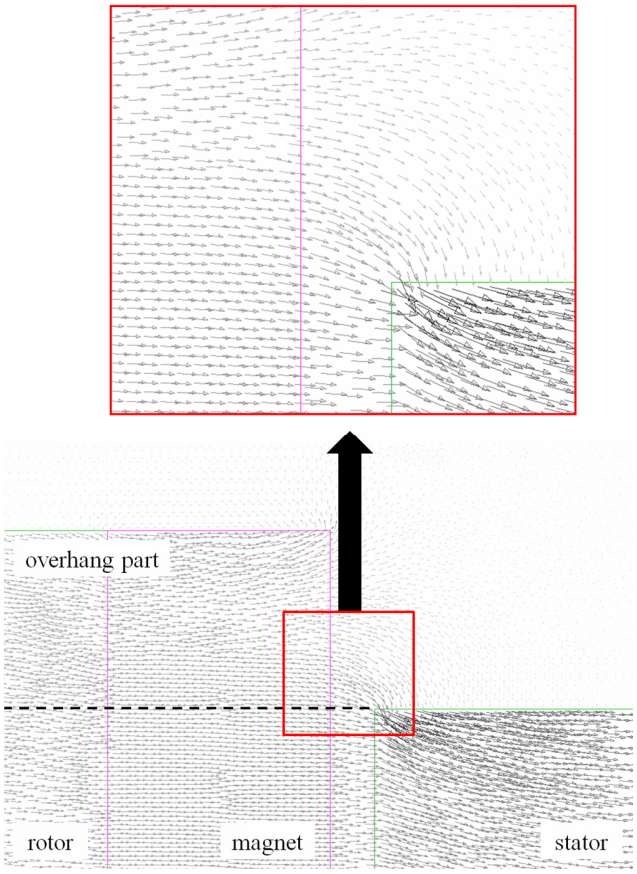

Fig. 6. Distribution of magnetic flux density by FEM

According to the flux division, the air-gap flux and the flux from the magnet can be derived as

$$\Phi_g = \frac{\Phi_r}{1+\left(\frac{R_g}{R_{mo}}\right)(1+2\eta+4\lambda)} \tag{21}$$

and

$$\Phi_m = \frac{1+\left(\frac{R_g}{R_{mo}}\right)(2\eta+4\lambda)}{1+\left(\frac{R_g}{R_{mo}}\right)(1+2\eta+4\lambda)} . \tag{22}$$

The air-gap flux density and the magnet flux density can be induced by

$$B_g = \frac{\frac{A_m}{A_g}}{1+\left(\frac{R_g}{R_{mo}}\right)(1+2\eta+4\lambda)} B_r \tag{23}$$

and

$$B_m = \frac{1+\left(\frac{R_g}{R_{mo}}\right)(2\eta+4\lambda)}{1+\left(\frac{R_g}{R_{mo}}\right)(1+2\eta+4\lambda)} B_r , \quad (24)$$

where

$$A_m = w_m \left(L_{st} + 2L_{oh}\right) \quad (25)$$

and

$$A_g = \left(w_m + w_f\right)\left(L_{st} + 2L_{oh}\right). \quad (26)$$

Table 1. Comparison between the analytical results and the FEM results of the motor employing ferrite magnets

Geometrical dimensions			Analytical results		3D FEM results		Difference*	
g (mm)	w_f (mm)	L_{oh} (mm)	B_m(T)	B_g(T)	B_m(T)	B_g(T)	B_m(%)	B_g(%)
0.5	5.0	0.0	0.356	0.281	0.353	0.279	-0.87	-0.76
0.5	5.0	7.0	0.352	0.276	0.343	0.272	-2.69	-1.50
0.5	5.0	10.0	0.350	0.273	0.336	0.267	-4.30	-2.28
0.5	4.0	0.0	0.356	0.292	0.354	0.290	-0.61	-0.89
0.5	4.0	7.0	0.352	0.287	0.344	0.282	-2.39	-1.62
0.5	4.0	10.0	0.350	0.284	0.337	0.278	-3.94	-2.40
1.0	5.0	0.0	0.326	0.249	0.321	0.249	-1.44	-0.24
1.0	5.0	7.0	0.321	0.243	0.313	0.243	-2.52	0.20
1.0	5.0	10.0	0.319	0.239	0.307	0.240	-3.62	0.21
1.0	4.0	0.0	0.326	0.259	0.322	0.258	-1.35	-0.35
1.0	4.0	7.0	0.321	0.252	0.314	0.252	-2.36	0.10
1.0	4.0	10.0	0.319	0.248	0.308	0.248	-3.43	0.13

At L_{st} =100.0 mm, h_m = 4.0 mm, w_m = 20.0 mm, μ_r = 1.05, and B_r = 0.40.

*: Difference = (3D FEM results – Analytical results) / 3D FEM results × 100.

Table 2. Comparison between the analytical results and the FEM results of the motor employing rare earth magnets

Geometrical dimensions			Analytical results		3D FEM results		Difference*	
g (mm)	w_f (mm)	L_{oh} (mm)	B_m(T)	B_g(T)	B_m(T)	B_g(T)	B_m(%)	B_g(%)
0.5	5.0	0.0	0.954	0.753	0.946	0.747	-0.85	-0.74
0.5	5.0	7.0	0.943	0.739	0.919	0.729	-2.68	-1.49
0.5	5.0	10.0	0.938	0.732	0.900	0.716	-4.28	-2.27
0.5	4.0	0.0	0.954	0.783	0.950	0.777	-0.47	-0.73
0.5	4.0	7.0	0.944	0.769	0.923	0.758	-2.24	-1.48
0.5	4.0	10.0	0.939	0.761	0.904	0.744	-3.80	-2.27
1.0	5.0	0.0	0.873	0.668	0.861	0.667	-1.44	-0.21
1.0	5.0	7.0	0.861	0.651	0.840	0.652	-2.50	0.23
1.0	5.0	10.0	0.854	0.641	0.824	0.643	-3.60	0.24
1.0	4.0	0.0	0.874	0.693	0.862	0.691	-1.32	-0.33
1.0	4.0	7.0	0.862	0.675	0.842	0.676	-2.34	0.12
1.0	4.0	10.0	0.855	0.665	0.827	0.666	-3.41	0.15

At L_{st} =100.0mm, h_m = 4.0mm, w_m = 20.0mm, μ_r = 1.0384, and B_r = 1.07.

*: Difference = (3D FEM results – Analytical results) / 3D FEM results × 100.

3. Results and Verification

For the verification of the proposed analytical model, the results from a FEM and the analytical results calculated from (23) and (24) are investigated. The investigations are conducted in various cases with different values of g, w_f and L_{oh}. Table 1 and Table 2 show the results for a motor employing ferrite magnets with B_r = 0.4 T and rare earth magnets with B_r = 1.07 T, respectively. B_m and B_g of FEM results is average value. B_m is calculated by averaging flux density in the middle of a magnet though rotor stack length. B_g is calculated by averaging flux density in the middle of the air gap though rotor stack length.

As shown in Table 1 and Table 2, there is little difference between results of the motor employing the ferrite magnet and the rare earth magnet. The accuracy of the EMCM is affected by L_{oh}. As the length of the overhang increase, the leakage flux at the end of the overhang is increased and the estimation of the magnetic flux path becomes difficult. This increases the difference between the analytical results and the FEM data. In cases in which L_{oh} is less than 7 mm, the differences of B_m and B_g are less than 3% and 2%, respectively. The differences of B_m and B_g are respectively less than 5% and 3% when L_{oh} is 10mm.

In the condition with same stator stack length, the total flux passing through air-gap increases when L_{oh} increases. However, the average flux densities B_m and B_g decline as the overhang increases, as shown in Table 1 and Table 2, this is because the area is more increased compared to the flux. In cases in which L_{st} is 100 mm, the total flux passing through the air gap increases by about 11% and 15% when L_{oh} is 7 mm and 10 mm, respectively.

4. Conclusion

This paper is noteworthy in that the time for design of SPM machines can be reduced remarkably via the reduction of time for initial design by using the proposed EMCM, which is analytical method considering overhang effects.

References

[1] S. I. Babic and C. Akyel, "Torque calculation between circular coils with inclined axes in air," *Int. J. Numer. Model.*, vol. 24, pp. 230-243, 2011.

[2] F. Baudart, E. Matagne, B. Dehez, and F. Labrique, "Analytical prediction of cogging torque in surface mounted permanent magnet motors," *Mathematics and Computers in Simulation*, vol. 90, pp. 205-217, 2013.

[3] W. P. Calixto, E. G. Marra, L. C. Brito, and B. P. Alvarenga, "A new methodology to calculate Carter factor using genetic algorithms," *Int. J. Numer. Model.*,

vol. 24, pp. 387-399, 2011.
[4] A. Chebak, P. Viarouge, and J. Cros, "Optimal design of a high-speed slotless permanent magnet synchronous generator with soft magnetic composite stator yoke and rectifier load," *Mathematics and Computers in Simulation*, vol. 81, pp. 239-251, 2010.
[5] F. Dubas, C. Espanet, and A. Miraoui, "An original analytical expression of the maximum magnet thickness in surface mounted permanent magnet motors," *Eur. Phys. J. Appl. Phys*., vol. 38, pp. 169-176, 2007.
[6] G. Gruosso and A. Brambilla, "Magnetic core model for circuit simulations including losses and hysteresis," *Int. J. Numer. Model*., vol. 21, pp. 309-334, 2008.
[7] D. Hanselman, *Brushless Permanent Magnet Motor Design*: 2nd ed., 2003, pp. 15-29.
[8] M. Hecquet, A. Ait-Hammouda, M. Goueygou, P. Brochet, and A. Randria, "Prediction of the electromagnetic noise of an asynchronous machine using experimental designs," *Mathematics and Computers in Simulation*, vol. 71, pp. 499-509, 2006.
[9] J. R. Hendershot and Jr., T. J. E. Miller, *Design of Brushless Permanent-Magnet Motors*: Oxford, U.K., 1994.
[10] M. F. Hsieh and Y. C. Hsu, "A generalized magnetic circuit modeling approach for design of surface permanent-magnet machines," *IEEE Trans. Ind. Electron*., vol. 59, pp. 779-792, 2012.
[11] F. N. Jurca and C. Martis, "Theoretical and experimental analysis of a three-phase permanent magnet claw-pole synchronous generator," *IET Electr. Power Appl*., vol. 6, pp. 491-503, 2012.
[12] Y. Kano, T. Kosaka, and N. Matsui, "Simple nonlinear magnetic analysis for permanent-magnet motors," *IEEE Trans. Ind. Appl*., vol. 41, pp. 1205-1214, 2005.
[13] G. Krebs, A. Tounzi, B. Pauwels, D. Willemot, and M. F. Piriou, "Design of a permanent magnet actuator for linear and rotary movements," *Eur. Phys. J. Appl. Phys*., vol. 44, pp. 77-85, 2008.
[14] P. Kurronen and J. Pyrhonen, "Analytic calculation of axial-flux permanent-magnet motor torque," *IET Electr. Power Appl*., vol. 1, pp. 59-63, 2007.
[15] G. Male, T. Lubin, S. Mezani, and J. Leveque, "Analytical calculation of the flux density distribution in a superconducting reluctance machine with HTS bulks rotor," *Mathematics and Computers in Simulation*, vol. 90, pp. 230-243, 2013.
[16] C. Mi, M. Filippa, W. Liu, and R. Ma, "Analytical method for predicting the air-gap flux of interior-type permanent-magnet machines," *IEEE Trans. Magn*., vol. 40, pp. 50-58, 2004.
[17] R. -B. Mignot, R. Glises, C. Espanet, E. S. Ellier, F. Dubas, and D. Chamagne, "Design of an axial flux PM motor using magnetic and thermal equivalent network," *Eur. Phys. J. Appl. Phys*., vol. 63, 30901, 2013.
[18] R. Qu and T. A. Lipo, "Analysis and modeling of air-gap and zigzag leakage fluxes in a surface-mounted permanent-magnet machine," *IEEE Trans. Ind. Appl*., vol. 40, pp. 121-127, 2004.
[19] A. Rahideh and T. Korakianitis, "Analytical magnetic field distribution of slotless brushless permanent magnet motors – Part I. Armature reaction field, inductance and rotor eddy current loss calculations," *IET Electr. Power Appl*., vol. 6, pp. 623-638, 2012.
[20] A. Rahideh and T. Korakianitis, "Analytical magnetic field distribution of slotless brushless PM motors. Part 2: Open-circuit field and torque calculations," *IET Electr. Power Appl*., vol. 6, pp. 639-651, 2012.
[21] J.S. Rho, C.H. Lee, T.K. Chung, C.H. Im, and H.K. Jung, "Analysis of a nanopositioning actuator using numerical and analytic methods," *IOP Smart Mater. Struct*., vol. 17, 025025, 2008.
[22] J.S. Ro, S.K. Hong, and H.K. Jung, "Characteristic analysis and design of a novel permanent magnet actuator for a vacuum circuit breaker," *IET Electr. Power Appl*., vol. 7, pp. 87-96, 2013.
[23] J. S. Ro, K. P. Yi, T. K. Chung, and H. K. Jung, "Characteristic analysis and shape optimal design of a ring-type traveling wave ultrasonic motor," *Eur. Phys. J. Appl. Phys*., vol. 63, 10901, 2013.
[24] J. S. Ro, K. P. Yi, T. K. Chung, and H. K. Jung, "Characteristic analysis of a traveling wave ultrasonic motor using a cylindrical dynamic contact model," *Journal of Electrical Engineering & Technology*, vol. 8, pp. 742-750, 2013.
[25] M. Ruba, I.-A. Viorel, and L. Szabo, "Modular stator switched reluctance motor for fault tolerant drive systems," *IET Electr. Power Appl*., vol. 7, pp. 159-169, 2013.
[26] P. Sewell, K. J. Bradley, J. C. Clare, P. W. Wheeler, A. Ferrah, and R. Magill, "Efficient dynamic models for induction machines," *Int. J. Numer. Model*., vol. 12, pp. 449-464, 1999.
[27] Y. Sofiane, A. Tounzi, and F. Piriou, "A non linear analytical model of switched reluctance machines," *Eur. Phys. J. Appl. Phys*., vol. 18, pp. 163-172, 2002.
[28] H. Tiegna, Y. Amara, and G. Barakat, "Overview of analytical models of permanent magnet electrical machines for analysis and design purposes," *Mathematics and Computers in Simulation*, vol. 90, pp. 162-177, 2013.
[29] J. P. Wang, D. K. Lieu, W. L. Lorimer, and A. Hartman, "Influence of the permanent magnet overhang on the performance of the brushless dc motor," *J. Appl. Phys*., vol. 83, pp. 6362-6364, 1998.
[30] L. J. Wu, Z. Q. Zhu, D. Staton, M. Popescu, and D. Hawkins, "Analytical prediction of electromagnetic performance of surface-mounted PM machines based on subdomain model accounting for tooth-tips," *IET Electr. Power Appl*., vol. 5, pp. 597-609, 2011.
[31] L. Zhu, S. Z. Jiang, Z. Q. Zhu, and C. C. Chan, "Analytical modeling of open-circuit air-gap field distributions in multisegment and multilayer interior permanent-magnet machines," *IEEE Trans. Magn*., vol. 45, pp. 3121-3130, 2009.

[32] Z. Q. Zhu, Y. Pang, D. Howe, S. Iwasaki, R. Deodhar, and A. Pride, "Analysis of electromagnetic performance of flux-switching permanent-magnet machines by nonlinear adaptive lumped parameter magnetic circuit model," *IEEE Trans. Magn*., vol. 41, pp. 4277-4287, 2005.

Han-Kyeol Yeo He received B.S. degree in electronic and electrical engineering from Sungkyunkwan University, Suwon, Korea, in 2012. He is currently working toward the Ph.D. degree in electrical engineering from the Seoul National University, Seoul, Korea. His current research interests include numerical analysis and design of electrical machines.

Dong-Kyun Woo He received B.S. degree in electrical engineering from Yonsei University, Seoul, Korea, in 2007. In 2014, he received a Ph.D. in electrical engineering from Seoul National University, Seoul, Korea, through the Combined Master's and Doctorate Program. Currently, he is carrying out research at Power & Industrial Systems R&D Center of Hyosung from 2014. His current research interests include numerical analysis and design of electrical machines.

Dong-Kuk Lim He received B.S. degree in the electrical engineering from Dongguk University, Seoul, Korea, in 2010. He is currently working toward the Ph.D. degree in electrical engineering and computer science from the Seoul National University, Seoul, Korea. His current research interests include design of electrical machines.

Jong-Suk Ro He received B.S. degree in mechanical engineering from Han-Yang University, Seoul, Korea, in 2001. In 2008, he earned a Ph.D. in electrical engineering from Seoul National University, Seoul, Korea, through the Combined Master's and Doctorate Program. He conducted research on cellular phone modules at R&D center of Samsung Electronics as a Senior Engineer from 2008 to 2012. From 2012 to 2013, he was at Brain Korea 21 Information Technology of Seoul National University as a Post-Doctoral Fellow. Currently, he is carrying out research at Electrical Energy Conversion System Research Division of Smart Grid Team at Korea Electrical Engineering & Science Research Institute as a Researcher.
His research interests are numerical analysis and optimal design of electric machines.

Hyun Kyo Jung (S'82-M'90-SM'99) He received the B.S., M.S., and Ph.D. degree in Electrical engineering from the Seoul National University, Seoul, Korea, in 1979, 1981, and 1984, respectively. From 1985 to 1994, he was a member of the faculty with Kangwon National University. From 1987 to 1989, he was with the Polytechnic University of Brooklyn, Brooklyn, NY. From 1999 to 2000, he was a Visiting Professor with the University of California at Berkeley. He is currently a Professor at the School of Electrical Engineering and Computer Science/Electrical Engineering, Seoul National University. His research interests are the analysis and design of the electric machine.